

Evaluation of Tris-Bipyridine Chromium Complexes for Flow Battery Applications: Impact of Bipyridine Ligand Structure on Solubility and Electrochemistry

Pablo J. Cabrera,^{†,§} Xingyi Yang,^{#,§,‡} James A. Suttill,^{†,§,‡} Rachel E. M. Brooner,^{†,§} Levi T. Thompson,^{*,#,§} and Melanie S. Sanford^{*,†,§}

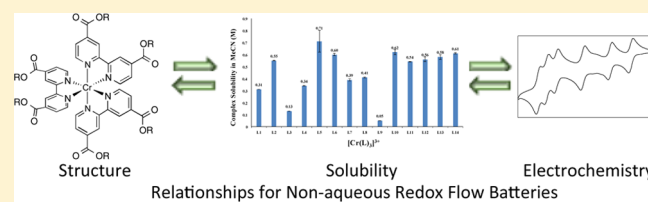
[†]Department of Chemistry, University of Michigan, 930 North University Avenue, Ann Arbor, Michigan 48109, United States

[#]Department of Chemical Engineering, University of Michigan, 2300 Hayward Street, Ann Arbor, Michigan 48109, United States

[§]Joint Center for Energy Storage Research (JCESR), Argonne, Illinois, United States

Supporting Information

ABSTRACT: This report describes the design, synthesis, solubility, and electrochemistry of a series of tris-bipyridine chromium complexes that exhibit up to six reversible redox couples as well as solubilities approaching 1 M in acetonitrile. We have systematically modified both the ligand structure and the oxidation state of these complexes to gain insights into the factors that impact solubility and electrochemistry. The results provide a set of structure–solubility–electrochemistry relationships to guide the future development of electrolytes for nonaqueous flow batteries. In addition, we have identified a promising candidate from the series of chromium complexes for further electrochemical and battery assessment.



INTRODUCTION¹

Redox flow batteries (RFBs) represent an emerging technology for use in grid scale energy storage applications.² In these systems, electrochemical energy is stored in solutions of redox active materials that are pumped between external electrolyte tanks across structured electrodes. The energy density of a RFB is dictated by eq 1, which has three main parameters: voltage window (V_{cell}), solubility (C_{active}), and number of electrons transferred (n).³

$$\hat{E} \propto 0.5 \times n \times V_{\text{cell}} \times C_{\text{active}} \times F \quad (1)$$

Aqueous RFBs are commercially available,⁴ and the most common electrolytes are solutions of vanadium salts.⁵ These offer the advantages of reversible electrochemistry, excellent cyclability, and high solubility (~ 2 M in H_2O). However, their energy densities are limited by the small voltage window of water (~ 1.2 V).^{2a,b,3} As a result, significant research effort over the last 15 years has focused on identifying redox active materials that can be used in solvents with wider voltage windows, such as acetonitrile or propylene carbonate.^{6–12} These nonaqueous solvents could enable large increases in V_{cell} and n , and thereby ultimately yield RFBs with significantly higher energy densities. Redox active materials for this application should meet at least five criteria. They should (1) undergo kinetically fast and chemically reversible redox reactions; (2) exhibit multiple reversible redox events over a large voltage window; (3) have high chemical, electrochemical, and cell-component stabilities in multiple charge (oxidation) states; (4) exhibit high solubility in multiple charge states; and

(5) be accessible from inexpensive, earth abundant starting materials.

In this context, metal coordination complexes (MCCs) have emerged as particularly promising candidates for use in nonaqueous RFBs. Examples of MCCs that have been studied previously are shown in Figure 1. These include acetylacetonate

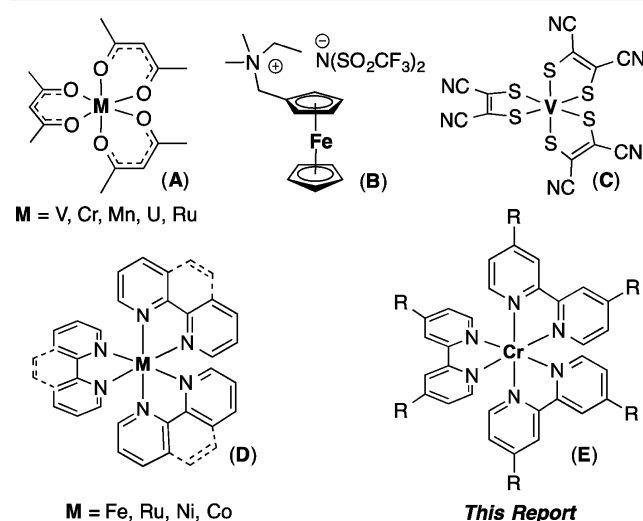


Figure 1. Representative examples of MCCs used in nonaqueous RFBs.

Received: June 12, 2015

complexes (A),¹⁰ metallocene derivatives (B),¹¹ dithiolate vanadium complexes (C),^{12a} and metal bipyridine and phenanthroline adducts (D).^{8,9} Complexes A–D meet many, but not all, of the five criteria. For instance, an alkylammonium ferrocene derivative (B)^{11a} was shown to undergo reversible redox reactions and exhibit high solubility (1.7 M in alkylcarbonate solvent mixtures). However, this material is limited to a single redox event ($n = 1e^-$) at 3.49 V versus Li/Li⁺, thus requiring the use of a low-potential redox active partner (often Li-metal), which leads to an increase in the complexity of the system and membrane design.

The majority of previous investigations of MCCs for RFB applications have focused on metal complexes bearing a single, commercially available ligand (e.g., acetylacetonate or 2,2'-bipyridine). As such, there are very few systematic studies of the impact of ligand structure and substitution on the solubility and redox properties of MCCs.^{10a,h} Such studies would provide structure–solubility–electrochemistry relationships that could be broadly useful for the design of new generations of MCCs for this application. A key objective of our program is to leverage our team's complementary expertise in synthetic inorganic chemistry and electrochemistry/battery engineering to delineate these structure–function relationships in prospective battery materials.

We report herein the design, synthesis, solubility, and electrochemical characterization of a series of bipyridine chromium complexes for use as electrolytes in nonaqueous RFBs. These complexes exhibit up to six redox couples over an approximately 2 V window¹³ and thus offer the potential for symmetric, multielectron cells (i.e., having the same active species in both half-cells of the battery).¹⁴ We demonstrate that the incorporation of substituents on the bipyridine ligands impacts the number of redox couples observed within the electrochemical window of acetonitrile as well as the position and reversibility of these couples. Furthermore, we show that changes to both ligand substituents and metal oxidation state have dramatic effects on solubility.

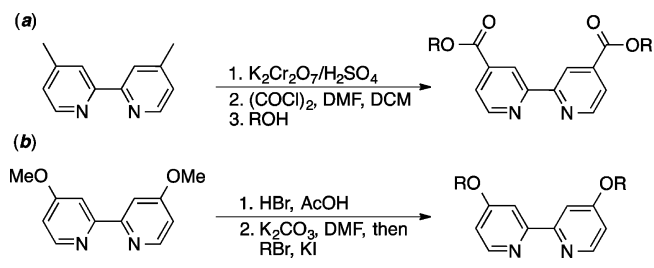
RESULTS AND DISCUSSION

Design and Synthesis of Metal Complexes. Our initial work focused on the synthesis of a range of air-stable ester-substituted bipyridine Cr³⁺ complexes. The ester substituent can be easily modified, thus enabling fast and scalable derivatization. We also synthesized the Cr⁰ analogues of several of these ester-bipyridine compounds. These Cr⁰ complexes represent another oxidation state accessed upon charging and discharging the flow battery. A previous report from our groups showed that the overall charge of a MCC has a large impact on solubility.¹⁴ Thus, we pursued a detailed investigation of the impact of ligand modifications on the solubility of both Cr³⁺ and Cr⁰ complexes. Finally, we synthesized and characterized a series of alkoxybipyridine Cr³⁺ complexes. We targeted these more electron-rich Cr³⁺ species to gain insights into the impact of ligand electronic properties on the solubility and electrochemistry of these systems.

The ester-bipyridine ligands were prepared via Jones oxidation of 4,4'-dimethylbipyridine to afford the corresponding dicarboxylic acid,¹⁵ which was further converted to the acid chloride by reaction with oxalyl chloride. Esterification with the corresponding alcohol afforded the desired ligands (L3–L14) in 31–67% yield over the three-step sequence (Scheme 1a).

The 4,4'-alkoxy-substituted bipyridine ligands were prepared by demethylation of 4,4'-dimethoxybipyridine with HBr,¹⁶

Scheme 1. Synthesis of Bipyridine Ligands (a) L3–L14 and (b) L16 and L17



followed by alkylation of the dihydroxybipyridine intermediate with the appropriate alkyl halide (Scheme 1b). Ligands L16 and L17 were obtained in 37% and 65% yield over these two steps, respectively.

Overall, 17 tris-bipyridyl Cr³⁺ complexes and 7 tris-bipyridyl Cr⁰ complexes were prepared in this study (Scheme 2). The Cr³⁺ complexes were obtained in 45–99% yield by stirring the appropriate ligand with [Cr(MeCN)₄](BF₄)₂ in acetonitrile for 15 min at room temperature, followed by 1e⁻ oxidation with AgBF₄ (Scheme 2a). The Cr⁰ complexes were prepared in 42–99% yield by refluxing the appropriate ligand with Cr(CO)₆ in degassed mesitylene under a nitrogen atmosphere (Scheme 2b). All of the metal complexes were characterized via elemental analysis and mass spectrometry. In addition, an X-ray crystal structure of [Cr(L15)₃]³⁺ was obtained, which shows an octahedral geometry with all Cr–N bond lengths in the range of 2.032–2.046 Å (Figure 2).

Solubility of Ester-bipyridine Cr³⁺ Complexes. We first assessed the solubility of [Cr(L1)₃]³⁺–[Cr(L14)₃]³⁺ in acetonitrile using UV–vis absorption spectroscopy. Acetonitrile was selected as the solvent based on its wide electrochemical window (~5 V) and low viscosity. The solubilities of the Cr³⁺ complexes derived from the commercially available bipyridine (L1) and 4,4'-dimethylbipyridine (L2) ligands were determined and used as benchmarks for comparison to the synthesized analogues. Solubility is a complicated phenomenon that involves the interplay of many, often competing, factors.¹⁷ Nonetheless, we initially hypothesized that three features of R were most likely to favorably impact the solubility of these complexes in acetonitrile: (1) longer chain length, (2) more chain branching, and (3) replacing –CH₂– groups with more electronegative atoms in the chain. We reasoned that increasing the chain length and branching could enhance solubility by disrupting packing in the solid state.¹⁷ In addition, we reasoned that replacing nonpolar –CH₂– groups with more polar atoms such as oxygen could increase solubility by enhancing favorable dipole–dipole interactions between the solute and the acetonitrile.

As summarized in Figure 3, the solubilities of the Cr³⁺ complexes of ligands L3–L14 range from 0.05 to 0.71 M. Increasing the alkyl chain length from one carbon ([Cr(L3)₃]³⁺) to four carbons ([Cr(L5)₃]³⁺)¹⁸ resulted in a >5-fold increase in solubility from 0.13 to 0.71 M. However, a further increase in the alkyl chain length to a seven carbon chain ([Cr(L7)₃]³⁺) led to a decrease in solubility relative to [Cr(L5)₃]³⁺ (0.39 M versus 0.71 M). The Cr complexes bearing seven and eight carbon chains had the same solubility (0.39 M for [Cr(L7)₃]³⁺ and [Cr(L8)₃]³⁺). We hypothesize that the lower solubility of [Cr(L7)₃]³⁺ and [Cr(L8)₃]³⁺ compared to [Cr(L5)₃]³⁺ may be due to the formation of a lipophilic shell around the more hydrophobic complexes, which

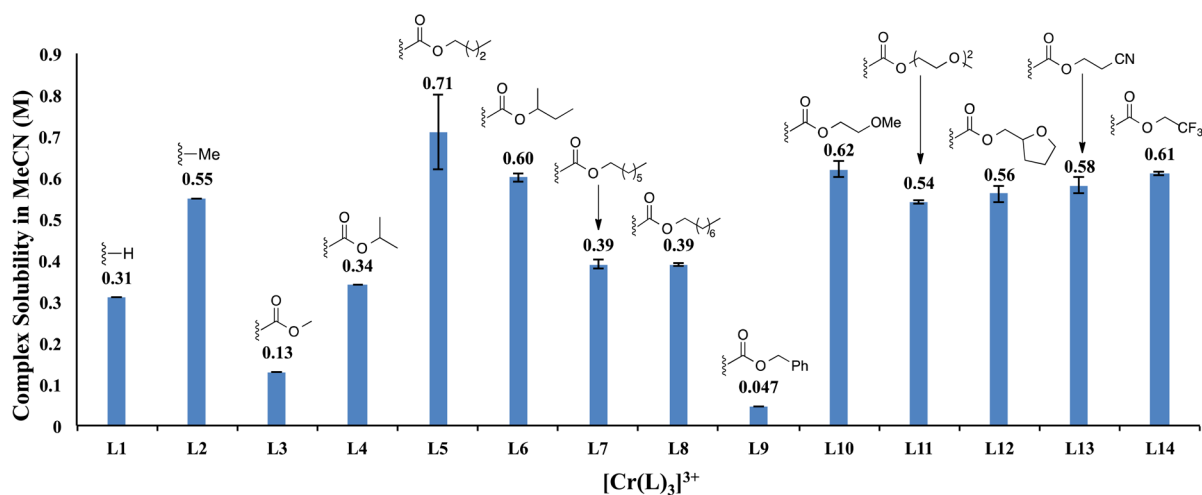


Figure 3. Solubility of $[\text{Cr}(\text{L})_3]^{3+}$ in acetonitrile.

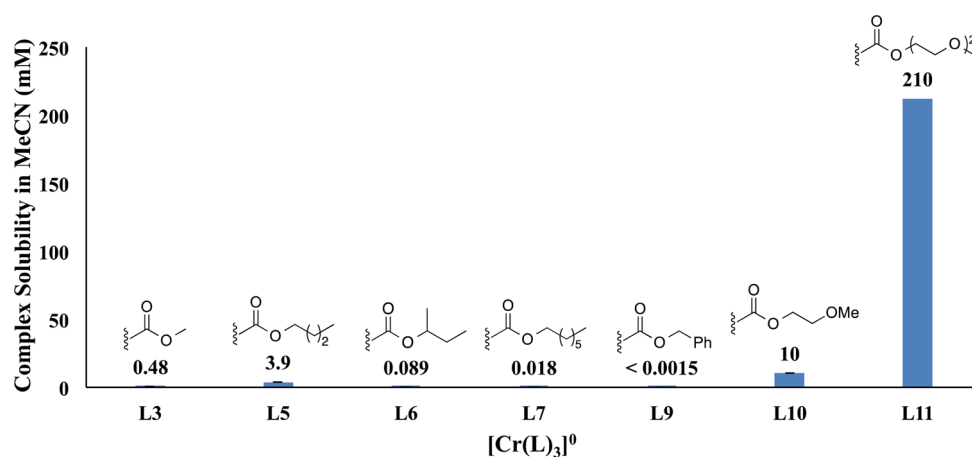


Figure 4. Solubility of $[\text{Cr}(\text{L})_3]^0$ in acetonitrile.

were also assessed. In these systems, the solubility in acetonitrile ranged from essentially insoluble (<0.0015 mM)¹⁹ to 210 mM (Figure 4). For all of the ligands examined, the neutral Cr^0 compounds were significantly less soluble than the corresponding cationic Cr^{3+} species. In the neutral complexes, moving from the one carbon chain in $[\text{Cr}(\text{L3})_3]^0$ to the four carbon butyl chain in $[\text{Cr}(\text{L5})_3]^0$ improved solubility by almost an order of magnitude (0.48 mM versus 3.9 mM, respectively). However, upon further increasing the alkyl chain length to a seven carbon chain ($[\text{Cr}(\text{L7})_3]^0$), a significantly lower solubility was observed (0.018 mM). Again, this may be due to the lipophilic nature of the heptyl chain.

The incorporation of a branched *sec*-butyl chain ($[\text{Cr}(\text{L6})_3]^0$) reduced the solubility of the complex as compared to the linear butyl chain (0.089 mM versus 3.9 mM, respectively). As discussed above, a similar decrease in solubility with branching was observed in the Cr^{3+} complexes, although the results for the neutral complex are more pronounced. The incorporation of the benzyl chain ($[\text{Cr}(\text{L9})_3]^0$) led to a complex that is essentially insoluble in acetonitrile (<0.0015 mM).¹⁹ This is likely due to the nonpolar nature of this substituent as well as stabilizing π - π stacking interactions of the aromatic units in the solid state.

The incorporation of electronegative atoms on the ester chains led to dramatic improvements in solubility compared to the aliphatic analogues. For example, moving from the butyl

chain ($[\text{Cr}(\text{L5})_3]^0$) to the methoxyethyl chain ($[\text{Cr}(\text{L10})_3]^0$) resulted in an ~ 3 -fold increase in solubility (3.9 versus 10 mM, respectively). Even more dramatically, moving from a heptyl chain ($[\text{Cr}(\text{L7})_3]^0$) to a methoxy(ethoxy)ethyl chain ($[\text{Cr}(\text{L11})_3]^0$) afforded an almost four order of magnitude enhancement in solubility (0.018 versus 210 mM, respectively).

Solubility of Alkoxybipyridine Cr^{3+} Complexes. The solubilities of the alkoxybipyridine Cr^{3+} complexes $[\text{Cr}(\text{L15})_3]^{3+}$ to $[\text{Cr}(\text{L17})_3]^{3+}$ were also determined in acetonitrile and range from 0.29 to 0.61 M (Figure 5). Ethers bearing methyl and butyl chains ($[\text{Cr}(\text{L15})_3]^{3+}$ and $[\text{Cr}(\text{L16})_3]^{3+}$) yielded compounds with similar solubilities (0.61 and 0.58 M, respectively). Somewhat surprisingly, the incorporation of the methyl ether diethylene glycol chain ($[\text{Cr}(\text{L17})_3]^{3+}$) resulted in a complex with only moderate solubility in acetonitrile (0.29 M). In general, the alkoxy-derived Cr^{3+} molecules reach a similar saturation point as the ester-bipyridine Cr^{3+} species.

Overall, these studies reveal two key points regarding solubility:

(1) There are significant differences in solubility (up to 4 orders of magnitude) between active species bearing the same supporting ligands but different oxidation states (i.e., Cr^{3+} versus Cr^0). This must be accounted for in nonaqueous RFB battery design and cycling.

(2) The solubility of these molecules is subject to a complicated interplay of factors. The solubility of Cr^{3+}

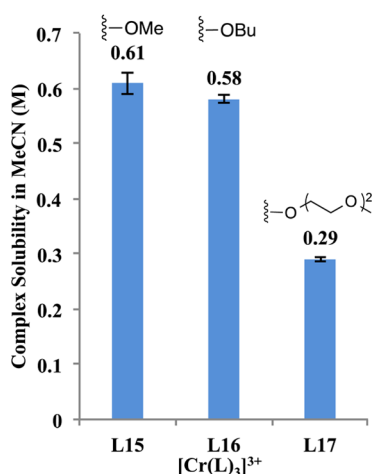


Figure 5. Solubility of functionalized alkoxy-bipyridine $[\text{Cr}(\text{L})_3]^{3+}$ in acetonitrile.

complexes is relatively insensitive to substituent effects (with values ranging from 0.2 to 0.7 M for most complexes). We hypothesize that the overall 3+ charge dominates the solubility properties of these molecules, rather than the specific substituents on the ligands. In contrast, the solubilities of the analogous neutral Cr^0 species varies over 4 orders of magnitude (~ 0.02 to 200 mM). At Cr^0 , the largest solubility enhancement was achieved by replacing nonpolar $-\text{CH}_2-$ groups with electronegative oxygen atoms on the ester side chains of the ligands.

Electrochemistry of Cr-Complexes. Cyclic voltammetry for all Cr^{3+} and Cr^0 complexes was performed in a three-electrode cell in acetonitrile with TBABF_4 as the supporting electrolyte and Ag/Ag^+ as the reference. Tables 1–4 list the redox potentials ($E_{1/2}$, average of the cathodic and anodic potentials), the peak current ratios after deconvolution ($i_p^{\text{red}}/i_p^{\text{ox}}$, ratio of cathodic current to anodic current), and the peak potential separation (ΔE_p , difference between cathodic and anodic potentials) for each of the complexes. The couple at the most positive potential is designated as the first redox couple (Figure 6A). A peak current ratio of 1 is indicative of a redox couple that is chemically reversible on the time scale of the CV experiment. It is important to note that these CV reversibility measurements do not necessarily correlate with cyclability in electrochemical evaluations over longer timeframes (e.g., charge–discharge). Nonetheless, CV serves as a useful method to conduct a rapid initial analysis of MCC electrochemistries.²⁰

The bipyridine $[\text{Cr}(\text{L1})_3]^{3+}$ and dimethylbipyridine $[\text{Cr}(\text{L2})_3]^{3+}$ complexes show six well-defined redox couples across 2.3 and 2.1 V, respectively (Table 1). When comparing the

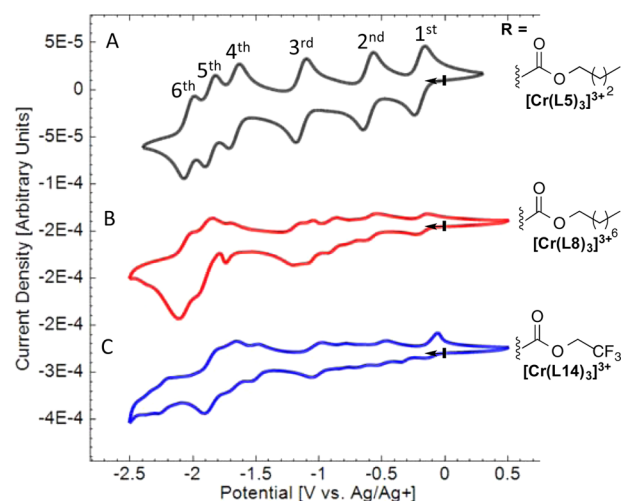


Figure 6. Cyclic voltammograms of a 10 mM solution of complex with 0.1 M TBABF_4 in acetonitrile. Reference is Ag/Ag^+ with AgBF_4 (0.01 M); working electrode is glassy carbon disk; counter electrode is platinum wire; scan rate is 100 mV s^{-1} ; temperature is 23°C . (A) $[\text{Cr}(\text{L5})_3]^{3+}$, (B) $[\text{Cr}(\text{L8})_3]^{3+}$, and (C) $[\text{Cr}(\text{L14})_3]^{3+}$. Bar indicates starting potential, and arrow indicates starting sweep direction.

redox potential ($E_{1/2}$) of the first couple of $[\text{Cr}(\text{L1})_3]^{3+}$ and $[\text{Cr}(\text{L2})_3]^{3+}$, we observe a significant shift toward a more negative potential with the more electron-donating methyl-substituted ligands (-0.56 V versus -0.72 V , respectively). These values are in accordance with those reported in the literature.²¹ When the complexes are cycled to potentials below -2.5 V , a new shoulder at approximately -1.4 V is observed. We attribute this shoulder to irreversible decomposition of the complexes. This indicates that only the first four redox couples are sufficiently stable to be considered for cycling in a RFB. Nevertheless, this chemistry could afford a symmetrical cell with $2e^-$ transfers at each electrode.

Complexes bearing the electron-withdrawing ester-substituted bipyridine ligands generally show six couples between -0.14 V and -2.05 V (Table 2 and Figure 6A). While the electronic structure of $\text{Cr}(\text{bpy})_3$ complexes in the various oxidation states is still the subject of significant debate,²² Wieghardt and co-workers have suggested that the redox events of these complexes are primarily ligand-centered.²³ Most modifications to the ester substituent have minimal impact on the electrochemistry (Table 2). For the majority of the ester bipyridine complexes, the first three redox couples (first, second, third) are spaced by approximately 0.5 V , whereas the last three redox couples are closer in potential, with a spacing of about 0.2 V .²⁴ This is consistent with previous literature reports

Table 1. Potentials, Peak Current Ratios, and Peak Separations for the Bipyridine Cr^{3+} and Dimethylbipyridine Cr^{3+} Complexes in Acetonitrile^a

compound		first	second	third	fourth	fifth	sixth
$[\text{Cr}(\text{L1})_3]^{3+}$	$E_{1/2}$ (V)	-0.56	-1.08	-1.65	-2.27	-2.58	-2.81
	$i_p^{\text{red}}/i_p^{\text{ox}}$	1.03	1.19	0.91	1.04	1.02	1.62
	ΔE_p (V)	0.084	0.077	0.077	0.077	0.084	0.084
$[\text{Cr}(\text{L2})_3]^{3+}$	$E_{1/2}$ (V)	-0.72	-1.22	-1.75	-2.34	-2.62	-2.84
	$i_p^{\text{red}}/i_p^{\text{ox}}$	0.94	0.98	0.94	1.04	1.05	2.11
	ΔE_p (V)	0.070	0.077	0.077	0.077	0.091	0.056

^aReference is Ag/Ag^+ with AgBF_4 (0.01 M); supporting electrolyte is TBABF_4 (0.1 M); working electrode is glassy carbon disk; counter electrode is platinum wire; scan rate is 100 mV s^{-1} ; temperature is 23°C .

Table 2. Potentials, Peak Current Ratios, and Peak Separations for the Ester-bipyridine Cr³⁺ Complexes in Acetonitrile^a

compound		first	second	third	fourth	fifth	sixth
[Cr(L3) ₃] ³⁺	<i>E</i> _{1/2} (V)	-0.20	-0.61	-1.14	-1.67	-1.86	-2.03
	<i>i</i> _p ^{red} / <i>i</i> _p ^{ox}	1.02	1.04	1.04	1.03	0.94	0.95
	Δ <i>E</i> _p (V)	0.070	0.070	0.077	0.063	0.056	0.056
[Cr(L4) ₃] ³⁺	<i>E</i> _{1/2} (V)	-0.17	-0.59	-1.22	-1.65	-1.85	-2.02
	<i>i</i> _p ^{red} / <i>i</i> _p ^{ox}	0.99	0.99	1.00	0.98	0.97	0.95
	Δ <i>E</i> _p (V)	0.060	0.060	0.065	0.060	0.045	0.050
[Cr(L5) ₃] ³⁺	<i>E</i> _{1/2} (V)	-0.20	-0.61	-1.14	-1.67	-1.86	-2.04
	<i>i</i> _p ^{red} / <i>i</i> _p ^{ox}	0.99	0.96	0.99	0.94	0.97	1.02
	Δ <i>E</i> _p (V)	0.072	0.078	0.080	0.071	0.066	0.069
[Cr(L9) ₃] ³⁺	<i>E</i> _{1/2} (V)	-0.17	-0.57	-1.11	-1.64	-1.82	-1.99
	<i>i</i> _p ^{red} / <i>i</i> _p ^{ox}	1.01	0.91	0.58	0.24	0.63	0.87
	Δ <i>E</i> _p (V)	0.078	0.078	0.070	0.083	0.066	0.072
[Cr(L10) ₃] ³⁺	<i>E</i> _{1/2} (V)	-0.14	-0.57	-1.13	-1.67	-1.89	-2.07
	<i>i</i> _p ^{red} / <i>i</i> _p ^{ox}	0.58	1.11	0.95	1.29	0.87	0.52
	Δ <i>E</i> _p (V)	0.13	0.11	0.11	0.12	0.12	0.14
[Cr(L11) ₃] ³⁺	<i>E</i> _{1/2} (V)	-0.17	-0.58	-1.12	-1.63	-1.82	-2.00
	<i>i</i> _p ^{red} / <i>i</i> _p ^{ox}	1.06	0.90	0.98	0.98	1.02	1.06
	Δ <i>E</i> _p (V)	0.084	0.070	0.084	0.063	0.056	0.070
[Cr(L12) ₃] ³⁺	<i>E</i> _{1/2} (V)	-0.21	-0.61	-1.15	-1.68	-1.87	-2.04
	<i>i</i> _p ^{red} / <i>i</i> _p ^{ox}	0.99	0.96	1.01	0.95	0.96	0.99
	Δ <i>E</i> _p (V)	0.093	0.094	0.10	0.093	0.092	0.096
[Cr(L13) ₃] ³⁺	<i>E</i> _{1/2} (V)	-0.17	-0.59	-1.12	-1.63	-1.83	-2.02
	<i>i</i> _p ^{red} / <i>i</i> _p ^{ox}	0.99	0.96	1.01	0.95	0.96	0.99
	Δ <i>E</i> _p (V)	0.14	0.13	0.13	0.14	0.14	0.14

^aReference is Ag/Ag⁺ with AgBF₄ (0.01 M); supporting electrolyte is TBABF₄ (0.1 M); working electrode is glassy carbon disk; counter electrode is platinum wire; scan rate is 100 mV s⁻¹; temperature is 23 °C.

Table 3. Potentials, Peak Current Ratios, and Peak Separations for the Alkoxy-bipyridine Cr³⁺ Complexes in Acetonitrile^a

compound		first	second	third	fourth	fifth	sixth
[Cr(L15) ₃] ³⁺	<i>E</i> _{1/2} (V)	-0.92	-1.36	-1.74	-2.30	-2.57	-2.80
	<i>i</i> _p ^{red} / <i>i</i> _p ^{ox}	0.70	0.79	0.65	0.75	0.92	0.47
	Δ <i>E</i> _p (V)	0.090	0.095	0.10	0.10	0.12	0.076
[Cr(L16) ₃] ³⁺	<i>E</i> _{1/2} (V)	-0.94	-1.38	-1.76	-2.31	-2.57	-2.79
	<i>i</i> _p ^{red} / <i>i</i> _p ^{ox}	0.98	0.98	1.00	0.97	1.00	0.25
	Δ <i>E</i> _p (V)	0.077	0.063	0.070	0.070	0.063	0.042
[Cr(L17) ₃] ³⁺	<i>E</i> _{1/2} (V)	-0.93	-1.37	-1.76	-2.30	-2.55	
	<i>i</i> _p ^{red} / <i>i</i> _p ^{ox}	0.87	1.03	0.90	1.01	0.73	
	Δ <i>E</i> _p (V)	0.070	0.070	0.077	0.063	0.077	

^aReference is Ag/Ag⁺ with AgBF₄ (0.01 M); supporting electrolyte is TBABF₄ (0.1 M); working electrode is glassy carbon disk; counter electrode is platinum wire; scan rate is 100 mV s⁻¹; temperature is 23 °C.

of related systems.¹³ Widely spaced redox events are desirable for RFB applications, since the potential window of the cell (*V*_{cell}) is determined by the spacing between the highest and lowest potential redox couple. In principle, the six redox couples associated with these ester-substituted bipyridine Cr complexes should enable a symmetrical 3*e*⁻ RFB cell in which a Cr⁰ complex is oxidized by 3*e*⁻ on one side of the cell and reduced by 3*e*⁻ on the other side of the cell.²⁵

A few ester substituents resulted in irreversible electrochemical behavior. For example, the cyclic voltammograms of complexes bearing *sec*-butyl ([Cr(L6)₃]³⁺), heptyl ([Cr(L7)₃]³⁺), and octyl chains ([Cr(L8)₃]³⁺) show large anodic currents at approximately -2.0 V (see Figure 6B for an example). These large increases in current could be due to ligand dissociation, as noted for other Cr(bpy)₃ complexes,²¹ or may be due to the formation of side products with high diffusivities. The cyclic voltammograms of the corresponding free bipyridine ligands show quasi-reversible peaks between -2

V and -2.5 V. The perfluorinated ester-containing complex [Cr(L14)₃]³⁺ also shows multiple irreversible redox events (Figure 6C). This is likely due to low stability of the fluorinated alkyl chains at highly reducing potentials.²⁶

For the alkoxy-substituted bipyridine Cr³⁺ complexes, the first reduction wave occurs at -0.9 V, which is significantly more negative than for the corresponding ester-derived complexes (Table 3). This is consistent with the resonance electron-donor properties of alkoxy substituents.²⁷ The complexes bearing alkoxy-substituted bipyridines show four quasi-reversible redox processes by cyclic voltammetry (Figure 7A). There is a decrease in the voltage separation between each redox couple relative to the analogous ester-substituted derivatives. At strongly reducing potentials (*V* > -2.5 V), the alkoxy-bipyridine complexes exhibit poor stability, which results in the observation of small shoulders (-1.59, -1.19, 0.84 V, Figure 7B). Additionally, the fifth peak in all of the alkoxy-bipyridine complexes has a larger peak current compared to the

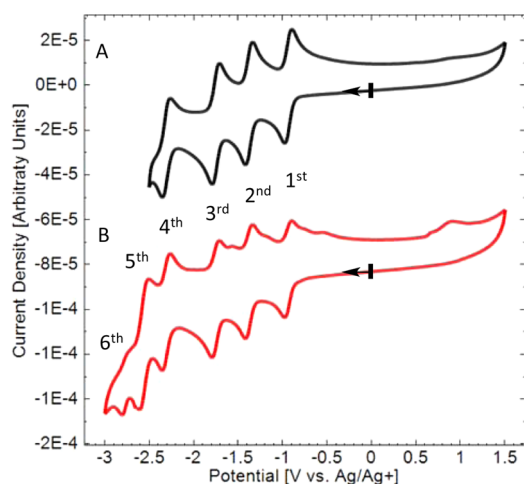


Figure 7. Cyclic voltammogram of a 10 mM solution of $[\text{Cr}(\text{L16})_3]^{3+}$ with 0.1 M TBABF_4 in acetonitrile. Reference is Ag/Ag^+ with AgBF_4 (0.01M); working electrode is glassy carbon disk; counter electrode is platinum wire; scan rate is 100 mV s^{-1} ; temperature is 23°C . (A) CV in black is for a voltage window of -2.5 to 1.5 V . (B) CV in red is for a voltage window of -3.0 to 1.5 V . Bar indicates starting potential and arrow indicates starting sweep direction.

other redox couples in the complex (Figure 7B). This increase in current may be related to free ligand in solution, as the voltammogram of free ligand shows a reversible redox couple at approximately -2.6 V . In the case of the ethylene glycol-substituted complex ($[\text{Cr}(\text{L17})_3]^{3+}$), the sixth peak is outside of the electrochemical window of acetonitrile (Table 3).

The cyclic voltammograms of the Cr^0 complexes are similar to those of the corresponding Cr^{3+} species (compare Figure 8A and Figure 8B). Six $1e^-$ couples are present at the same potentials as their Cr^{3+} analogues (Table 4). The first three redox couples are widely spaced ($\sim 0.5 \text{ V}$), whereas the last three peaks (fourth, fifth, sixth) are closer in potential ($\sim 0.2 \text{ V}$).

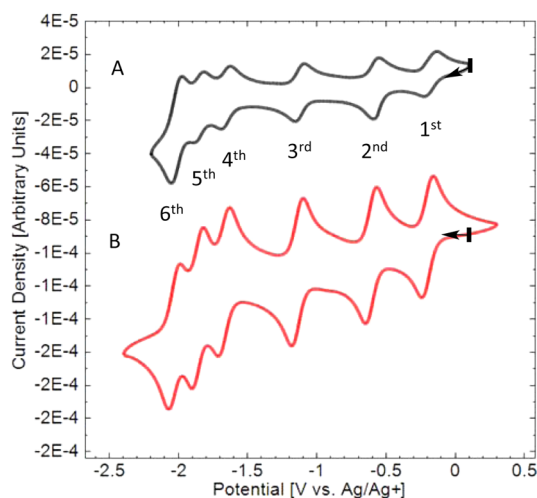


Figure 8. (A) Cyclic voltammogram in black for a saturated solution of $[\text{Cr}(\text{L5})_3]^0$ ($\sim 3.85 \text{ mM}$) with 0.1 M TBABF_4 in acetonitrile.²⁸ (B) Cyclic voltammogram in red for a 10 mM solution of $[\text{Cr}(\text{L5})_3]^{3+}$ with 0.1 M TBABF_4 in acetonitrile. Reference is Ag/Ag^+ with AgBF_4 (0.01M); working electrode is glassy carbon disk; counter electrode is platinum wire; scan rate is 100 mV s^{-1} ; temperature is 23°C . Bar indicates starting potential and arrow indicates starting sweep direction.

The sixth redox couple shows a large peak current as compared to the others. Interestingly, analogous behavior is not observed in the Cr^{3+} series. The reason for this increase in peak current is unclear, but it might be due to the generation and reduction of the free ester-bipyridine ligand.²¹ Overall, the neutral complexes show less reversible peaks than those of the Cr^{3+} complexes based on their peak current ratios. Notably, the low solubility of the neutral complexes in acetonitrile requires that the CV experiments be performed near saturation limits. This leads to low peak currents compared to the double layer current (background current). As a consequence of their low solubility in acetonitrile, the Cr^0 compounds bearing *sec*-butyl, heptyl, and benzyl ester substituents ($[\text{Cr}(\text{L6})_3]^0$, $[\text{Cr}(\text{L7})_3]^0$, and $[\text{Cr}(\text{L9})_3]^0$) could not be characterized by CV.

Overall, the cyclic voltammetry studies revealed two key points for the development of new redox active MCCs for flow battery applications:

(1) Alterations to the MCC ligand backbone can significantly impact the reversibility of the redox events as well as the stability of the metal complex toward reduction. Most ester-substituted bipyridine complexes maintain six reversible redox couples; however, the incorporation of long aliphatic chains or perfluorinated substituents results in molecules with irreversible redox behavior and poor electrochemical stability.

(2) The electronic properties of the ligand lead to significant changes in the stability of the complexes, number of accessible redox couples, and cell potential. The MCCs derived from bipyridine ligands bearing electron-donating substituents (H, alkoxy and methyl) show lower stability at highly reducing potentials (below -2.5 V), and they provide access to just four stable redox couples across 1.4 V . In contrast, most of the ester-substituted complexes exhibit enhanced electrochemical stability at low potentials and provide six reversible redox couples across $\sim 2 \text{ V}$ window.

CONCLUSIONS

This report describes a systematic study of the impact of bipyridine ligand substitution on the solubility and cyclic voltammetry of $\text{Cr}(\text{bpy})_3$ complexes. These studies show that solubility in the Cr^0 state is currently the limiting factor for achieving high energy densities. However, this solubility can be enhanced by 4 orders of magnitude through the incorporation of ester substituents bearing polar oxygen atoms. These substituents have minimal impact on the electrochemical behavior (as measured by cyclic voltammetry). On the basis of all of these investigations, complex $[\text{Cr}(\text{L11})_3]^0$ was selected as a particularly promising candidate to move forward to more advanced battery testing.¹⁴ Our initial studies (reported independently) have shown that an unoptimized H-cell containing $[\text{Cr}(\text{L11})_3]^0$ is capable of accessing four of the six available redox couples (two redox couples at each electrode).¹⁴

As such, complex $[\text{Cr}(\text{L11})_3]^0$ can be compared directly to the alkylammonium ferrocene derivative **B**,^{11a} which is among the most promising MCC RFB active species reported to date. Compound **B** is approximately 8-fold more soluble than $[\text{Cr}(\text{L11})_3]^0$ (1.7 M versus 0.2 M , respectively). Compound **B** also has higher stability than $[\text{Cr}(\text{L11})_3]^0$, as it can be cycled over 100 times without significant capacity fade. In contrast, $[\text{Cr}(\text{L11})_3]^0$ begins to fade after ~ 10 cycles in an H-cell.¹⁴

However, $[\text{Cr}(\text{L11})_3]^0$ offers several key advantages relative to **B**. Complex **B** participates in a single one-electron transfer event, and as such, it can only be used as one side of an asymmetric $1e^-$ RFB ($n = 1$). In contrast, $[\text{Cr}(\text{L11})_3]^0$ enables

Table 4. Potentials, Peak Current Ratios, and Peak Separations for the Ester-bipyridine Cr⁰ Complexes in Acetonitrile^a

compound		first	second	third	fourth	fifth	sixth
[Cr(L3)] ₃ ⁰	$E_{1/2}$ (V)	-0.18	-0.59	-1.12	-1.65	-1.83	-2.01
	$i_p^{\text{red}}/i_p^{\text{ox}}$	1.56	0.95	1.02	1.12	0.34	1.20
	ΔE_p (V)	0.049	0.051	0.054	0.052	0.050	0.049
[Cr(L5)] ₃ ⁰	$E_{1/2}$ (V)	-0.18	-0.58	-1.13	-1.66	-1.85	-2.02
	$i_p^{\text{red}}/i_p^{\text{ox}}$	0.99	0.83	0.98	0.96	1.08	0.96
	ΔE_p (V)	0.077	0.047	0.064	0.059	0.049	0.059
[Cr(L10)] ₃ ⁰	$E_{1/2}$ (V)	-0.17	-0.58	-1.12	-1.64	-1.82	-2.00
	$i_p^{\text{red}}/i_p^{\text{ox}}$	0.92	1.04	0.91	0.71	1.00	0.89
	ΔE_p (V)	0.061	0.061	0.070	0.078	0.070	0.085
[Cr(L11)] ₃ ⁰	$E_{1/2}$ (V)	-0.18	-0.58	-1.11	-1.63	-1.82	-2.00
	$i_p^{\text{red}}/i_p^{\text{ox}}$	1.3	1.22	1.13	1.06	0.98	1.32
	ΔE_p (V)	0.065	0.062	0.067	0.072	0.059	0.078

^aReference is Ag/Ag⁺ with AgBF₄ (0.01 M); supporting electrolyte is TBABF₄ (0.1 M); working electrode is glassy carbon disk; counter electrode is platinum wire; scan rate is 100 mV s⁻¹; temperature is 23 °C.

the construction of a symmetrical RFB in which two or three electron transfers occur on each side of the cell (i.e., $n = 2$ or 3). As shown in eq 1, a doubling or tripling of n results in a doubling or tripling of the energy density compared to an RFB with $n = 1$. The symmetric battery configuration (with the same complex on both sides of the cell) offers the additional advantage of mitigating irreversible performance erosion by crossover of active species between the two sides of the cell.²⁹

The advantages associated with complexes of general structure [Cr(L11)]₃⁰ should motivate future work aimed at further enhancing the solubility and electrochemical stability of these and related MCCs.³⁰ With advances in these two areas, MCCs that exhibit multielectron transfer events hold considerable promise as active species for nonaqueous RFBs.

ASSOCIATED CONTENT

Supporting Information

The Supporting Information is available free of charge on the ACS Publications website at DOI: 10.1021/acs.inorgchem.5b01328.

Experimental procedures and characterization of all new compounds including spectroscopic and potentiometric data (PDF)

X-ray crystallographic data of [Cr(L15)]₃³⁺ (CIF)

AUTHOR INFORMATION

Corresponding Authors

*(L.T.T.) E-mail: ltt@umich.edu.

*(M.S.S.) E-mail: mssanfor@umich.edu.

Author Contributions

[‡]X.Y. and J.A.S. contributed equally.

Notes

The authors declare no competing financial interest.

ACKNOWLEDGMENTS

This work was supported as part of the Joint Center for Energy Storage Research, an Energy Innovation Hub funded by the U.S. Department of Energy, Office of Science, Basic Energy Sciences. We gratefully acknowledge Dr. Jeff Kampf for X-ray crystallographic analysis of [Cr(L15)]₃³⁺, as well as funding from NSF Grant CHE-0840456 for X-ray instrumentation.

REFERENCES

- List of abbreviations: MCC = metal coordination complex; RFB = redox flow battery; V_{cell} = voltage window; C_{active} = solubility; n = number of electrons transferred; F = Faraday's constant; \tilde{E} = energy density; CV = cyclic voltammetry; V = voltage; i = current; TBABF₄ = tetrabutylammonium tetrafluoroborate; bpy = bipyridine; $E_{1/2}$ = half-wave potential; $i_p^{\text{red}}/i_p^{\text{ox}}$ = peak current ratio; ΔE_p = peak potential separation.
- (a) Yang, Z.; Zhang, J.; Kintner-Meyer, C. W.; Lu, X.; Choi, D.; Lemmon, J. P.; Liu, J. *Chem. Rev.* **2011**, *111*, 3577. (b) Alotto, P.; Guarnieri, M.; Moro, F. *Renewable Sustainable Energy Rev.* **2014**, *29*, 325. (c) Dunn, B.; Kamath, H.; Tarascon, J.-M. *Science* **2011**, *334*, 928. (d) Weber, A. Z.; Mench, M. M.; Meyers, J. P.; Ross, P. N.; Gostick, J. T.; Liu, Q. *J. Appl. Electrochem.* **2011**, *41*, 1137.
- (a) Ponce de León, C.; Frías-Ferrer, A.; González-García, J.; Szánto, D. A.; Walsh, F. C. *J. Power Sources* **2006**, *160*, 716. (b) Huang, Q.; Wang, Q. *ChemPlusChem* **2015**, *80*, 312.
- (a) Wang, W.; Luo, Q.; Li, B.; Wei, X.; Li, L.; Yang, Z. *Adv. Funct. Mater.* **2013**, *23*, 970.
- (a) Skyllas-Kazacos, M.; Chakrabarti, M. H.; Hajimolana, S. A.; Mjalli, F. S.; Saleem, M. *J. Electrochem. Soc.* **2011**, *158*, R55.
- (a) Brushett, F. R.; Vaughney, J. T.; Jansen, A. N. *Adv. Energy Mater.* **2012**, *2*, 1390. (b) Li, Z.; Li, S.; Liu, S.; Huang, K.; Fang, D.; Wang, F.; Peng, S. *Electrochem. Solid-State Lett.* **2011**, *14*, A171. (c) Kaur, A. P.; Holubowitch, N. E.; Ergun, S.; Elliott, C. F.; Odom, S. A. *Energy Technology* **2015**, *3*, 476. (d) Huang, J.; Cheng, L.; Assary, R. S.; Wang, P.; Xue, Z.; Burrell, A. K.; Curtiss, L. A.; Zhang, L. *Adv. Energy Mater.* **2015**, *5*, 1401782. (e) Wei, X.; Xu, W.; Huang, J.; Zhang, L.; Walter, E.; Lawrence, C.; Vijayakumar, M.; Henderson, W. A.; Liu, T.; Cosimbescu, L.; Li, B.; Sprenkle, V.; Wang, W. *Angew. Chem., Int. Ed.* **2015**, *54*, 8684. (f) Oh, S. H.; Lee, C. W.; Chun, D. H.; Jeon, J. D.; Shim, J.; Shin, K. H.; Yang, J. H. *J. Mater. Chem. A* **2014**, *2*, 19994.
- (a) Wang, W.; Xu, W.; Cosimbescu, L.; Choi, D.; Li, L.; Yang, Z. *Chem. Commun.* **2012**, *48*, 6669. (b) Wei, X.; Xu, W.; Vijayakumar, M.; Cosimbescu, L.; Liu, T.; Sprenkle, V.; Wang, W. *Adv. Mater.* **2014**, *26*, 7649. For semisolid redox active electrolytes for nonaqueous RFBs, see: (c) Duduta, M.; Ho, B.; Wood, V. C.; Limthongkul, P.; Brunini, V. E.; Carter, W. C.; Chiang, Y.-M. *Adv. Energy Mater.* **2011**, *1*, 511. (d) Hamelet, S.; Larcher, D.; Dupont, L.; Tarascon, J.-M. *J. Electrochem. Soc.* **2013**, *160*, A516. (e) Hamelet, S.; Tzedakis, T.; Leriche, J.-B.; Sailer, S.; Larcher, D.; Taberna, P.-L.; Simon, P.; Tarascon, J.-M. *J. Electrochem. Soc.* **2012**, *159*, A1360. (f) Youssry, M.; Madec, L.; Soudan, P.; Cerbelaud, M.; Guyomard, D.; Lestriez, B. *Phys. Chem. Chem. Phys.* **2013**, *15*, 14476. For polyoxometalates for nonaqueous RFBs, see: (g) Pratt, H. D., III; Hudak, N. S.; Fang, X.; Anderson, T. M. *J. Power Sources* **2013**, *236*, 259. (h) Pratt, H. D., III; Anderson, T. M. *Dalton Trans.* **2013**, *42*, 15650.

- (8) Nonaqueous systems MCCs bearing bipyridine or phenanthroline ligands: (a) Matsuda, Y.; Morita, T. M.; Tanaka, K.; Okada, M.; Matsumura-Inoue, T. *Denki Kagaku* **1985**, *53*, 632. (b) Matsuda, Y.; Tanaka, K.; Okada, M.; Takasu, Y.; Morita, M.; Matsumura-Inoue, T. *J. Appl. Electrochem.* **1988**, *18*, 909. (c) Morita, M.; Tanaka, Y.; Tanaka, K.; Matsuda, Y.; Matsumura-Inoue, T. *Bull. Chem. Soc. Jpn.* **1988**, *61*, 2711. (d) Mun, J.; Lee, M.-J.; Park, J.-W.; Oh, D.-J.; Lee, D.-Y.; Doo, S.-G. *Electrochem. Solid-State Lett.* **2012**, *15*, A80. (e) Chakrabarti, M. H.; Dryfe, R. A. W.; Roberts, E. P. L. *Electrochim. Acta* **2007**, *52*, 2189. (f) Kim, J.-H.; Kim, K. J.; Park, M.-S.; Lee, N. J.; Hwang, U.; Kim, H.; Kim, Y.-J. *Electrochem. Commun.* **2011**, *13*, 997. (g) Chakrabarti, M. H.; Lindfield Roberts, E. P.; Saleem, M. *Int. J. Green Energy* **2010**, *7*, 445. (h) Xing, X.; Zhang, D.; Li, Y. *J. Power Sources* **2015**, *279*, 205. (i) Park, M.-S.; Lee, N. J.; Lee, S.-W.; Kim, K. J.; Oh, D.-J.; Kim, Y.-J. *ACS Appl. Mater. Interfaces* **2014**, *6*, 10729.
- (9) Patents about nonaqueous RFBs MCCs bearing bipyridine based ligands: (a) Maly-Schreiber, B.; Whitehead, A. H. W.O. Patent 101284, September 13, 2007. (b) Sun, H.; Park, J.; Lee, D.; Son, S. (Samsung Electronics Co., Ltd., KR). U.S. Patent 0195283, August 11, 2011. (c) Lee, M. J.; Lee, D.; Oh, D.; Park, J.; Hwang, S. (Samsung Electronics Co., Ltd., KR). U.S. Patent 0107661, May 3, 2012. (d) Lee, M.; Oh, D.; Hwang, S. (Samsung Electronics Co., Ltd., KR). Redox Flow Battery. U.S. Patent 0171530, July 5, 2012. (e) Park, J.; Lee, M.; Lee, D.; Oh, D. (Samsung Electronics Co., Ltd., KR). Redox Flow Battery. U.S. Patent 0171541, July 5, 2012. (f) Mun, J.; Hwang, S.; Lee, D.; Kim, Y.; Kwon, O.; Yim, T. (KRKR, Seoul National University R&DB Foundation Samsung Electronics Co., Ltd., KRKR, Seoul National University R&DB Foundation Samsung Electronics Co., Ltd.). Electrolyte for Redox Flow Battery and Redox Flow Battery Including the Same. U.S. Patent 004819, January 3, 2013. (g) Park, J.; OH, D.; Lee, D.; Lee, M. (Samsung Electronics Co., Ltd., KR). Organic Electrolyte Solution and Redox Flow Battery Including the Same. U.S. Patent 196,206, August 1, 2013. (h) Park, J.; OH, D.; Lee, D.; Lee, M. (Samsung Electronics Co., Ltd., KR). Redox Flow Battery. U.S. Patent 193,687, July 10, 2014.
- (10) Nonaqueous MCCs bearing acetylacetonate ligands: (a) Yamamura, T.; Shiokawa, Y.; Yamana, H.; Moriyama, H. *Electrochim. Acta* **2002**, *48*, 43. (b) Liu, Q.; Sleightholme, A. E. S.; Shinkle, A. A.; Li, Y.; Thompson, L. T. *Electrochem. Commun.* **2009**, *11*, 2312. (c) Sleightholme, A. E. S.; Shinkle, A. A.; Liu, Q.; Monroe, C. W.; Thompson, L. T.; Li, Y. *J. Power Sources* **2011**, *196*, 5742. (d) Shinkle, A. A.; Sleightholme, A. E. S.; Thompson, L. T.; Monroe, C. W. *J. Appl. Electrochem.* **2011**, *41*, 1191. (e) Zhang, D.; Liu, Q.; Shi, X.; Li, Y. *J. Power Sources* **2012**, *203*, 201. (f) Shinkle, A. A.; Sleightholme, A. E. S.; Griffith, L. D.; Thompson, L. T.; Monroe, C. W. *J. Power Sources* **2012**, *206*, 490. (g) Zhang, D.; Lan, H.; Li, Y. *J. Power Sources* **2012**, *217*, 199. (h) Suttill, J. A.; Kucharyanu, J. F.; Escalante-Garcia, I. L.; Cabrera, P. J.; James, B. R.; Savinell, R. F.; Sanford, M. S.; Thompson, L. T. *J. Mater. Chem. A* **2015**, *3*, 7929.
- (11) Nonaqueous systems MCCs based on metallocene ligands: (a) Wei, X.; Cosimbescu, L.; Xu, W.; Hu, J. Z.; Vijayakumar, M.; Feng, J.; Hu, M. Y.; Deng, X.; Xiao, J.; Liu, J.; Sprenkle, V.; Wang, W. *Adv. Energy Mater.* **2015**, *5*, 1400678. (b) Hwang, B.; Park, M.-S.; Kim, K. *ChemSusChem* **2015**, *8*, 310. (c) Zhao, Y.; Ding, Y.; Song, J.; Li, G.; Dong, G.; Goodenough, J. B.; Yu, G. *Angew. Chem., Int. Ed.* **2014**, *53*, 11036. (d) Park, K.; Cho, J. H.; Shanmuganathan, K.; Song, J.; Peng, J.; Gobet, M.; Greenbaum, S.; Ellison, C. J.; Goodenough, J. B. *J. Power Sources* **2014**, *263*, 52.
- (12) (a) Cappillino, P. J.; Pratt, H. D., III; Hudak, N. S.; Tomson, N. C.; Anderson, T. M.; Anstey, M. R. *Adv. Energy Mater.* **2014**, *4*, 1300566. (b) Anderson, T. M.; Anstey, M.; Tomson, N. C. (Sandia Co., US) U.S. Patent 20140239906, August 28, 2014.
- (13) McDaniel, A. M.; Tseng, H.-W.; Damrauer, N. H.; Shores, M. P. *Inorg. Chem.* **2010**, *49*, 7981.
- (14) Cabrera, P. J.; Yang, X.; Suttill, J. A.; Hawthorne, K. L.; Brooner, R. E. M.; Sanford, M. S.; Thompson, L. T. *J. Phys. Chem. C* **2015**, *119*, 15882.
- (15) Hoertz, P. G.; Staniszewski, A.; Marton, A.; Higgins, G. T.; Incarvito, C. D.; Rheingold, A. L.; Meyer, G. J. *J. Am. Chem. Soc.* **2006**, *128*, 8234.
- (16) Hong, Y.-R.; Gorman, C. B. *J. Org. Chem.* **2003**, *68*, 9019.
- (17) (a) Anslyn, E. V.; Dougherty, D. A. *Modern Physical Organic Chemistry*, 1st ed.; University Science Books: CA, 2005; p 153–202. (b) Palmer, D. S.; Llinàs, A.; Morao, I.; Day, G. M.; Goodman, J. M.; Glen, R. C.; Mitchell, J. B. O. *Mol. Pharmaceutics* **2008**, *5*, 266.
- (18) With complex $[\text{Cr}(\text{L}5)_3]^{3+}$, the relatively large error resulted from the high viscosity of the saturated solution.
- (19) Solubility estimated based on the lower detection limit of the Nandrop UV-vis spectrometer (2 ng/mL).
- (20) In principle, differences in the chain length of the ligand (and thus molecular size) could impact the electron transfer kinetics and diffusion (and thus limit power densities of a battery). However, in previous work with $\text{M}(\text{acac})_3$ complexes (see ref 10h), we found small differences in the diffusion coefficient of complexes with varying ligand chain lengths, which were all within an acceptable range for RFB applications (see ref 2d). These results suggest that this is unlikely to be a problem in the current systems.
- (21) (a) Sato, Y.; Tanaka, N. *Bull. Chem. Soc. Jpn.* **1969**, *42*, 1021. (b) Hughes, M. C.; Rao, J. M.; Macero, D. J. *Inorg. Chim. Acta* **1979**, *35*, L321.
- (22) For a discussion of the electronic structure of $[\text{M}(\text{bpy})_3]$ complexes see: (a) Creutz, C. *Comments Inorg. Chem.* **1982**, *1*, 293. (b) König, E.; Herzog, S. *J. Inorg. Nucl. Chem.* **1970**, *32*, 585. For IR studies on low oxidation states of $[\text{Cr}(\text{bpy})_3]$ suggesting that the bpy ligand is negatively charged see: (c) Saito, Y.; Takemoto, J.; Hutchinson, B.; Nakamoto, K. *Inorg. Chem.* **1972**, *11*, 2003. For a discussion of the electronic structure of $[\text{Cr}(\text{bpy})_3]^{+2}$: (d) Cotton, F. A.; Wilkinson, G.; Murillo, C. A.; Bochmann, M. *Advanced Inorganic Chemistry*, 6th ed.; Wiley & Sons: New York, 1999; p 822. For a discussion of the formal oxidation state of the metal center in $[\text{Cr}(\text{bpy})_3]^{+3}$ and $[\text{Cr}(\text{bpy})_3]^{+2}$: (e) Wilkinson, G.; Gillard, R. D.; McCleverty, J. A. *Comprehensive Coordination Chemistry*, 1st ed.; Pergamon Press: Oxford, 1987; Vol. 3, p 712. For the synthesis and characterization of $[\text{Cr}(\text{bpy})_3]^{+2}$ and $[\text{Cr}(\text{bpy})_3]^{+1}$: (f) Hein, F. V.; Herzog, S. *Z. Anorg. Allg. Chem.* **1952**, *267*, 337. For the synthesis and characterization of $[\text{Cr}(\text{bpy})_3]^{0}$: (g) Herzog, S.; Schon, W. Z. *Anorg. Allg. Chem.* **1958**, *297*, 323. (h) Behrens, H.; Müller, A. Z. *Anorg. Allg. Chem.* **1965**, *341*, 124. (i) Quirk, J.; Wilkinson, G. *Polyhedron* **1982**, *1*, 209. For the synthesis and characterization of $[\text{Cr}(\text{bpy})_3]^x$ ($x = -1, -2, -3$) see: Herzog, S.; Grimm, U.; Waicenbauer, W. Z. *Chem.* **1967**, *7*, 355.
- (23) Scarborough, C. C.; Sproules, S.; Weyhermüller, T.; DeBeer, S.; Wiegardt, K. *Inorg. Chem.* **2011**, *50*, 12446.
- (24) For RFB applications, it is important that these closely spaced redox events be reversible. If one of them is not, decomposition can occur via disproportionation.
- (25) In practice, we have been able to demonstrate charge-discharge in a symmetrical cell with $n = 2e^-$ with complex $[\text{Cr}(\text{L}11)_3]^{0}$. See ref 14.
- (26) Barker, D. J.; Brewin, D. H.; Dahm, R. H.; Hoy, L. R. *J. Electrochim. Acta* **1978**, *23*, 1107.
- (27) (a) Carey, F. A.; Sundberg, R. J. *Advanced Organic Chemistry: Part A: Structure and Mechanisms*, 3rd ed.; Plenum Press: New York, 1991; pp 197–208. (b) Tucker, J. W.; Stephenson, C. R. J. *J. Org. Chem.* **2012**, *77*, 1617.
- (28) The cyclic voltammogram of $[\text{Cr}(\text{L}5)_3]^{0}$ shown in Figure 8 is the third full scan. See the SI for full details on the CV analysis.
- (29) Currently, the most common membranes used for nonaqueous RFBs are anion exchange membranes, such as Neosepta AHA and AMI-7001. However, these are not very effective at preventing cross-over. For membrane developments in nonaqueous RFBs see: Shin, S.-H.; Yun, S.-H.; Moon, S.-H. *RSC Adv.* **2013**, *3*, 9095.
- (30) Long-term stability of the redox active species is an important factor for the development of RFBs. We have conducted a solution stability study for complex $[\text{Cr}(\text{L}11)_3]^{0}$. A saturated solution of the complex was diluted in acetonitrile and stored for 24 h. UV-vis

absorption spectroscopy demonstrated unchanged spectral data suggesting that no decomposition occurs during that time-scale (see [Supporting Information](#) for details).